

## Acknowledgements

We acknowledge with appreciation the unfailing support of the non-crystalline diffraction group (particularly Dr. E. Towns-Andrews and Mrs. Sue Slawson) and the detector group (particularly Dr. R. Lewis) at the Daresbury Synchrotron Radiation Source. This work has been supported by the BBSRC, the MRC, the Wellcome Trust and the British Heart Foundation.

## References

- [1] Harford, J.J. and Squire, J.M., *Biophys. J.* (1996) **50**, 145-155.
- [2] Harford, J.J. and Squire, J.M., *Biophys. J.* (1992) **63**, 387-396.
- [3] Hudson, L., PhD Thesis (1996), University of London.
- [4] Hudson, L., Harford, J.J., Denny, R.C. and Squire, J.M., *J. Mol. Biol.* **273**, 440-455.
- [5] Rayment, I., *et al.*, *Science* (1993) **261**, 50-58.
- [6] Dominguez, R., Freyzon, Y., Trybus, K.M. and Cohen, C., *Cell* (1998) **94**, 559-571.
- [7] Kabsch, K., Mannherz, H.G., Suck, D., Pai, E.F. and Holmes, K.C., *Nature* (1990) **347**, 37-44.
- [8] <http://www.dl.ac.uk/SRS/CCP13>
- [9] Squire, J.M., *Curr. Opin. Struct. Biol.* (1997) **7**, 247-257.
- [10] Harford, J.J. and Squire, J.M., *Rep. Prog. Phys.* (1997) **60**, 1723-1787.
- [11] Harford, J.J., *et al.* and Squire, J.M., in *Proceedings of Hakone Muscle Symposium* (Eds Sugi and Pollack) (Plenum Press, 1998).
- [12] Squire, J.M., in *Current Methods in Muscle Physiology* (Ed. H. Sugi) (Oxford University Press, 1998) **241-285**.
- [13] Irving, M., *et al.*, *Nature* (1995) **375**, 688-691.
- [14] Dobbie, I., *et al.*, and Irving, M., *Nature* (1998) **396**, 383-387.
- [15] Reedy, M.K., *J. Mol. Biol.* (1968) **31**, 155-176.
- [16] Hudson, L., Denny, R.C., Harford, J.J., Reedy, M.K., Irving, T.C. and Squire, J.M. (in preparation).
- [17] Squire, J.M. and Harford, J.J., *J. Mus. Res. Cell Motil.* (1988) **9**, 344-358.
- [18] Whittaker, M., Wilson-Kubalek, E.M., Smith, J.E., Faust, L., Milligan, R.A. and Sweeney, H.L., *Nature* (1995) **378**, 748-751.

## Microphase separation in Poly(oxyethylene)-Poly(oxybutylene) Diblock copolymers

S.M. Mai<sup>1</sup>, J.P.A. Fairclough<sup>2</sup>, N.J. Terrill<sup>3</sup>, S.C. Turner<sup>2</sup>, I.W. Hamley<sup>4</sup>, M.W. Matsen<sup>5</sup>, A.J. Ryan<sup>2,3</sup> and C. Booth<sup>1</sup>

<sup>1</sup> Department of Chemistry, University of Manchester, Manchester, M13 9PL, U.K.

<sup>2</sup> Department of Chemistry, University of Sheffield, Sheffield, S3 7HF, U.K.

<sup>3</sup> CLRC Daresbury Laboratory, Daresbury, Warrington, Cheshire WA4 4AD, U.K.

<sup>4</sup> School of Chemistry, University of Leeds, Leeds, LS2 9JT, U.K.

<sup>5</sup> Polymer Science Centre, University of Reading, Whiteknights, Reading, RG6 6AF, U.K.

## Introduction

Diblock copolymers with narrow block length distributions may be readily prepared by sequential anionic polymerisation of ethylene oxide followed by 1,2-butylene oxide. We denote these copolymers  $E_mB_n$ , where E represents an oxyethylene unit  $[OCH_2CH_2]$  and B an oxybutylene unit  $[OCH_2CH(CH_2CH_3)]$ . Their bulk properties are of significant interest, since microphase-separated structures may form from the disordered melt when the temperature is lowered, either by crystallisation of the E blocks<sup>1-3</sup>, or by microphase separation in the melt state<sup>4</sup>.

## Experimental Procedure

Diblock copolymers were prepared by sequential anionic polymerisation of ethylene oxide (EO) followed by 1,2-butylene oxide (BO). Details of the methods have been published<sup>4</sup>. Characterisation of the intermediate poly(oxyethylene) and the final copolymer was by gel permeation chromatography (GPC) and <sup>13</sup>C NMR spectroscopy.

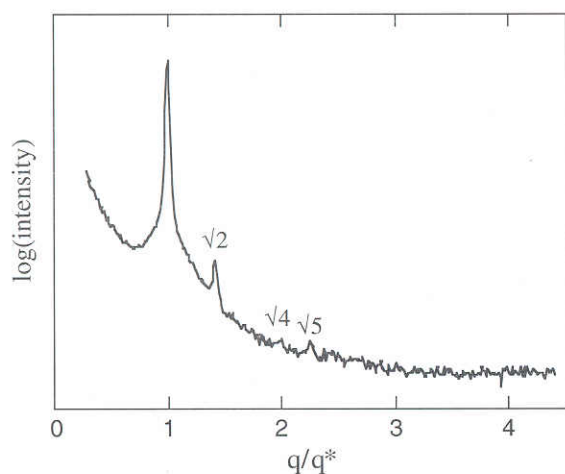
## Time Resolved Small-Angle X-Ray Scattering

SAXS measurements were carried out on Beamline 8.2 of the SRS, Daresbury Laboratory, Warrington, UK<sup>6</sup>. The loaded pans were placed in the cell of a Linkam DSC of single-pan design. Samples were heated from room temperature to  $T_{ODT} + 30$  °C at 10 °C min<sup>-1</sup>, held at the maximum temperature for 1 min

and cooled at  $10\text{ }^{\circ}\text{C min}^{-1}$  to  $10\text{ }^{\circ}\text{C}$ . The data acquisition system had a time-frame generator which collected the data in 6 s frames separated by a wait-time of  $10\text{ }\mu\text{s}$ .

### Microphase Structures and Order-Disorder Transition Temperatures

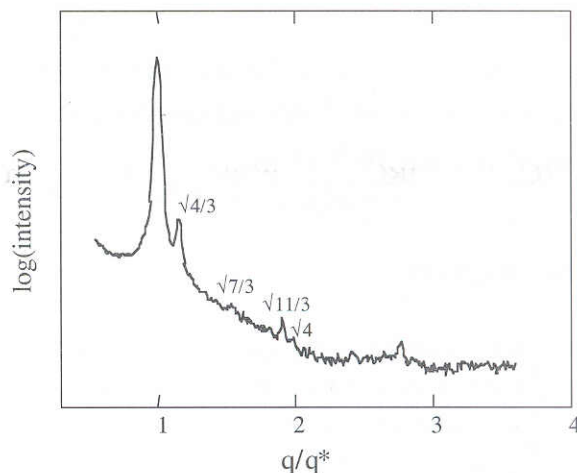
Figures 1 and 2 show SAXS patterns from copolymer melts which illustrate the cubic phase with  $\text{Im}\bar{3}\text{m}$  symmetry (body-centred cubic, bcc) of copolymer  $\text{E}_{40}\text{B}_{79}$  at  $35\text{ }^{\circ}\text{C}$  and the bicontinuous cubic phase with  $\text{Ia}\bar{3}\text{d}$  symmetry (gyroid, gyr) of copolymer  $\text{E}_{75}\text{B}_{54}$  at  $70\text{ }^{\circ}\text{C}$ . The data are presented as  $\log(\text{intensity})$  versus normalized wave vector,  $q/q^*$ , where  $q^*$  is the value of  $q$  at the peak of the first-order reflection.



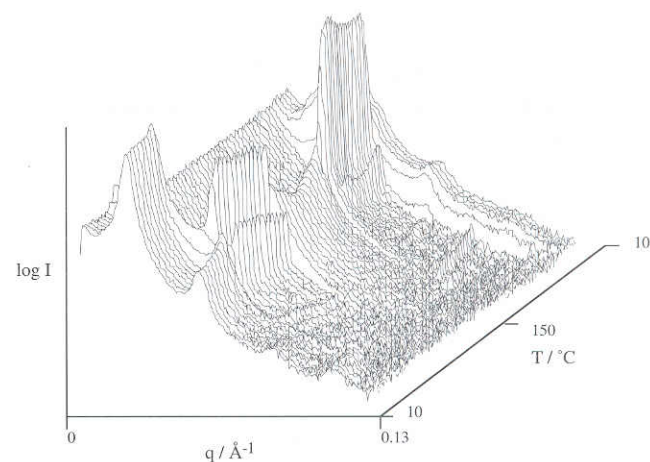
**Figure 1:** SAXS patterns for the molten copolymer  $\text{E}_{40}\text{B}_{79}$  at  $35\text{ }^{\circ}\text{C}$ .  $q^*$  is the value of  $q$  at the peak of the first order reflection. The logarithmic intensity scale is arbitrary. Reflections at  $q/q^* = 1, \sqrt{2}, \sqrt{4}$  and  $\sqrt{5}$  indicate a body-centred cubic phase.

Figure 3 shows a time-resolved SAXS schematic of the phase behaviour of copolymer  $\text{E}_{75}\text{B}_{54}$  obtained during heating and cooling the copolymer. At low temperature there are four equally spaced reflections which is consistent with a lamellar semicrystalline phase, at intermediate temperatures ( $63\text{ }^{\circ}\text{C} - 126\text{ }^{\circ}\text{C}$ ) the gyroid phase is observed (see Figure 2), while the broad scattering peak at high temperatures ( $T > 126\text{ }^{\circ}\text{C}$ ) indicates a disordered melt with composition fluctuations. The phase sequence is reversed on cooling. Heating and cooling experiments, such as illustrated in Figure 3, were used to locate the temperature of the order-disorder transition (ODT). In fact, as described previously<sup>4</sup>, the ODT was defined not only from the step change in the peak-

maximum intensity (see Figure 3), but also from the step changes in peak width and peak shape.



**Figure 2:** SAXS patterns for the molten copolymer  $\text{E}_{75}\text{B}_{54}$  at  $70\text{ }^{\circ}\text{C}$ .  $q^*$  is the value of  $q$  at the peak of the first order reflection. The logarithmic intensity scale is arbitrary. Reflections at  $q/q^* = 1, \sqrt{4/3}, \sqrt{7/3}, \sqrt{11/3}$  and  $\sqrt{12/3}$  indicate a gyroid phase.



**Figure 3:** Three-dimensional relief diagram of time-resolved SAXS data obtained with a time resolution of 6 s while heating and cooling copolymer  $\text{E}_{75}\text{B}_{54}$ . The plot shows  $\log(\text{intensity})$  versus scattering vector,  $q$ , versus temperature,  $T$ . The thermal cycle was  $10\text{ }^{\circ}\text{C} \rightarrow 150\text{ }^{\circ}\text{C} \rightarrow 10\text{ }^{\circ}\text{C}$  at a ramp rate of  $10\text{ }^{\circ}\text{C min}^{-1}$ .

### Temperature dependence of $\chi$

To locate the copolymers on the conventional phase diagram ( $\chi N_v$  versus  $\phi_E$ ), the value of  $\chi$  is formulated using the accumulated data for symmetrical copolymers ( $\phi_E = 0.5$ ) as a function of temperature  $\chi = B/T + A$ . The approximation for  $\chi$  was evaluated from the mean-field approximation for its critical value ( $\chi N_v = 10.5$ ) for microphase separation produced by Leibler<sup>7</sup>, which gives

$$\chi = 48.0/T - 0.0535$$

The value of  $\chi$  was also evaluated using the fluctuation correction by Fredrickson and Helfand<sup>8</sup> (Figure 4)

$$\chi N_v = 10.5 + 41N^{-1/3}, N = r_v b^6 \rho^2$$

with approximate values for the statistical segment length ( $b \approx 5.3 \times 10^{-10}$  m) and number density ( $\rho \approx 1.4 \times 10^{28}$  m<sup>-3</sup>), which gives

$$\chi = 75.6/T - 0.0929$$

## Phase Diagram

The results from the samples were used to define the phase boundaries shown in Figure 4, which is plotted with  $\chi$  calculated for the fluctuating melt. The filled circles denote order-disorder transitions (ODT) while the open circles signify order-order transitions (OOT). With an increase in  $\chi N_v$  (i.e., on cooling) and with the exception of the gyroid phase, all structured phases persisted to the crystal-liquid boundary. Lines are drawn on the phase diagram in order to highlight the features.

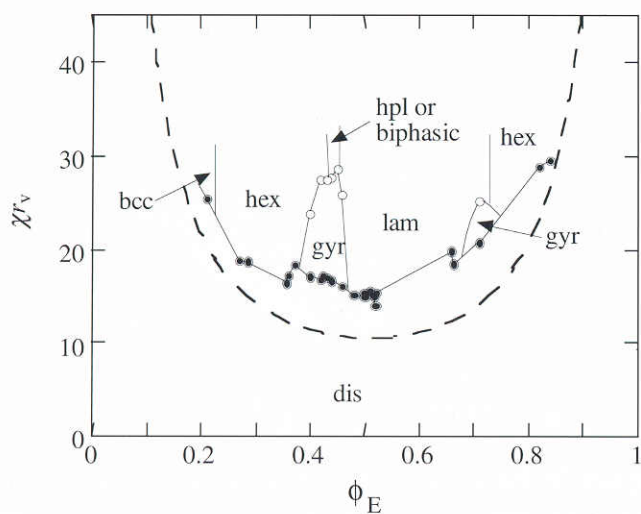


**Figure 4:** Phase diagram ( $\chi N_v$  versus  $\phi_E$ ) constructed using  $\chi$  calculated for the fluctuating melt. The filled circles denote order-disorder transitions (ODT) and the open circles order-order transitions (OOT). The solid curves have been drawn to indicate the different phases observed, but do not correspond to precise phase boundaries. The dashed curve is the boundary predicted by self-consistent mean-field theory.

The phase diagram is asymmetric about  $\phi_E = 0.5$ . If  $\chi$  is independent of  $\phi_E$ , the global symmetry of the phase diagram is controlled by the conformational asymmetry parameter,  $\varepsilon$ , where

$$\varepsilon = (v_E b_B^2 / v_B b_E^2)$$

where  $v_E$ ,  $v_B$ ,  $b_E$  and  $b_B$  represent the volumes and

statistical lengths of the E and B blocks. Only if  $\varepsilon = 1$  can the phase diagram be symmetrical. For this E/B system  $\varepsilon = 0.65^{1,4}$  and this effect is to bias the phase diagram to the high  $\phi_E$  side.

Figure 4 shows that the ODT boundary is not smooth, particularly between the disordered and gyroid phase which occurs at a higher  $\chi N_v$  than would be required for a smooth boundary between the lamellar and hexagonal regions. This reflects the lower ODT temperature observed for the gyroid phase than the lamellar or hexagonal phase formed from a copolymer with the same segment length. Figure 4 also shows the theoretical predictions (dashes) predicted by self-consistent field theory<sup>7,9,10</sup>. Theory predicts  $\chi N_v = 10.5$  at  $\phi_E = 0.5$  compared with  $\chi N_v = 14$  for the experimental boundary. Mean-field theory has not yet been generalized to account for composition fluctuations. However, the difference between experiment and theory is in part forced because allowance was made for a fluctuating melt when treating experimental data to calculate  $\chi$ .

## References

- [1] Yang, Y.-W., Tanodekaew, S., Mai, S.-M., Booth, C., Ryan, A. J., Bras, W. and Viras, K., *Macromolecules* (1995), **28**, 6029.
- [2] Ryan, A. J., Fairclough, J. P. A., Hamley, I. W., Mai, S.-M. and Booth, C., *Macromolecules* (1997), **30**, 1723.
- [3] Mai, S.-M., Fairclough, J. P. A., Viras, K., Gorry, P. A., Hamley, I. W., Ryan, A. J. and Booth, C., *Macromolecules* (1997), **30**, 8392.
- [4] Mai, S.-M., Fairclough, J. P. A., Hamley, I. W., Matsen, M. W., Denny, R.C., Liao, B.-X., Booth, C. and Ryan, A. J., *Macromolecules* (1996) **29**, 6212.
- [5] Bras, W., Derbyshire, G. E., Ryan, A. J., Mant, G.R., Felton, A., Lewis, R.A., Hall, C.J. and Greaves, G.N., *Nuclear Instruments and Methods in Physics Research* (1993) **A326**, 587.
- [6] Bras, W., Derbyshire, G. E., Clarke, S., Devine, A., Komanschek, B. U., Cooke, J. and Ryan, A.J., *J. Appl. Cryst.* (1994), **35**, 4537.
- [7] Leibler, L., *Macromolecules* (1980) **13**, 1602.
- [8] Fredrickson, G.H. and Helfand, E., *J. Chem. Phys.* (1987) **87**, 697.
- [9] Matsen, M.W. and Schick, M., *Phys. Rev. Lett.* (1994) **72**, 2660.
- [10] Matsen, M.W. and Bates, F.S., *Macromolecules* (1996) **29**, 1091.